

# Simulation on Surface Tracking Pattern using the Dielectric Breakdown Model

Jun-Won Kim\* and Young-Su Roh†

**Abstract** – The tracking pattern formed on the dielectric surface due to a surface electrical discharge exhibits fractal structure. In order to quantitatively investigate the fractal characteristics of the surface tracking pattern, the dielectric breakdown model has been employed to numerically generate the surface tracking pattern. In dielectric breakdown model, the pattern growth is determined stochastically by a probability function depending on the local electric potential difference. For the computation of the electric potential for all points of the lattice, a two-dimensional discrete Laplace equation is solved by mean of the successive over-relaxation method combined to the Gauss-Seidel method. The box counting method has been used to calculate the fractal dimensions of the simulated patterns with various exponent  $\eta$  and breakdown voltage  $\phi_b$ . As a result of the simulation, it is found that the fractal nature of the surface tracking pattern depends strongly on  $\eta$  and  $\phi_b$ .

**Keywords:** Surface tracking, Fractal, Dielectric breakdown model, Successive over-relaxation method, Box counting method

## 1. Introduction

When the surface of a dielectric material is electrically deteriorated due to environmental factors such as moisture and dust, a leakage current may flow along the surface between electrodes to which a rated voltage is applied. Continuous flowing of leakage currents lead to surface tracking which can be described as a mixed process of discharge inception, carbonization, carbon path propagation and molecular decomposition of the insulating material. [1] Since the surface tracking pattern is determined by the conducting channels of leakage currents, the carbonization pattern on the surface of an organic insulating material is one of essential factors to verify an electrical fire due to the leakage current. [2, 3]

The carbonized surface tracking pattern on the dielectric material due to the leakage current exhibits a branching and self-similar pattern. Such pattern is too complicated to be analyzed by conventional Euclidean geometry. It is well known that the general topological characteristics of dielectric breakdown, such as surface discharges and electrical trees, are of a fractal nature. Fractals have an excellent capability of expressing naturally occurring phenomena and shapes to which conventional and existing mathematical models are inadequate. [4-5] Many researches have been carried out on the fractal characteristics of various dielectric breakdowns. These include, for example, the fractal nature of creeping discharge patterns of solid insula-

tors [4], the fractal dimensions of tracking patterns of gamma irradiated ethylene propylene diene monomer [5], fractals for partial discharge recognition [6], and the fractal analysis of electrical trees [7].

In this paper, a numerical study is performed on the formation and growth of the surface tracking along the dielectric surface using the dielectric breakdown model (DBM). DBM is known to be a macroscopic mathematical model combining the diffusion-limited aggregation model [8] with electric field. DBM was developed by Niemeyer, Pietronero, and Weismann in 1984. [9] After numerical generation of the surface tracking based on DBM, tracking patterns are theoretically examined in terms of fractal dimensions. The box counting method is employed to calculate the fractal dimension.

This paper is organized as follows. The next section involves a brief description of the characteristics of an organic insulating material carbonized by a leakage current. In Sec. 3, the numerical computation to simulate surface tracking patterns based on DBM is presented. In Sec. 4, surface tracking patterns are analyzed using the box counting method. Finally, the conclusion of the paper is presented in Sec. 5.

## 2. Carbonization Pattern of a Phenolic Resin

Fig. 1 shows the configuration of electrodes and a phenolic resin specimen to make carbonized surface tracking patterns. A detailed description of the experimental setup regarding Fig. 1 has been presented in [3]. Here, a voltage of AC 220 V is applied between electrodes on the Bakelite

† Corresponding author: Dept. of Electrical and Electronic Engineering, Soongsil University, Korea. (yroh@ssu.ac.kr)

\* Dept. of Electrical and Electronic Engineering, Soongsil University, Korea. (your79jw@naver.com)

plate with the surface contaminated by salt water. Bakelite is a kind of phenolic resin which is one of the most popular organic insulating materials for low voltage. Fig. 2 illustrates the formation process of the carbonized conducting path on the Bakelite surface, which has been photographed by a high speed camera. As can be seen, the surface discharge grows as time passes.

Carbonized surface tracking patterns obtained in the experiment are presented in Fig. 3. Here, the two patterns are apparently different although they are created under the same experimental condition because the pattern growth is determined stochastically by the local electric potential difference. Consequently, the branched conducting channels of the pattern propagate in random directions until the main conducting path of the pattern is generated between electrodes. It seems that a large number of thin conducting channels are branched from the major thick channels in a self-similar form, thereby making the pattern to be of a fractal nature. Such fractal structure can be confirmed in Fig. 4.

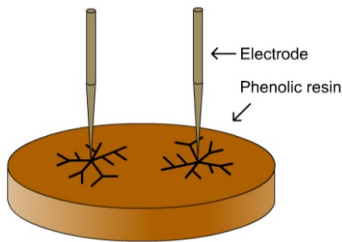


Fig. 1. Electrodes and a phenolic resin specimen to make carbonized surface tracking patterns. [3]

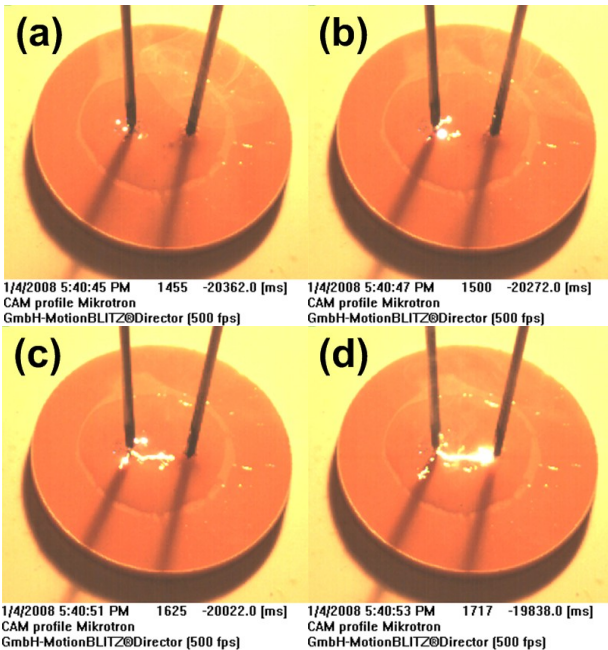


Fig. 2. The formation process of the carbonized conducting path on the surface of a phenolic resin. [3]

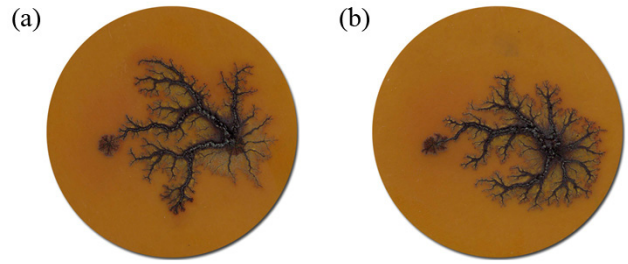


Fig. 3. Carbonized surface tracking patterns on the surfaces of Bakelite plates due to tracking



Fig. 4. A magnified carbonized surface tracking pattern photographed by an optical microscope.

### 3. Numerical Generation of Surface Tracking Patterns using DBM

#### 3.1 Dielectric Breakdown Method

In the DBM method [9, 10], a two-dimensional square lattice is used to simulate dielectric breakdown and the discharge pattern grows stepwise, starting from an electrode with electric potential  $\phi = 0$  V, and ending at the other electrode of which potential is normalized to be 1 V for computational simplicity. The discharge pattern is equivalent to the surface tracking pattern discussed in this paper. The electric potential is determined for all points of the lattice by solving the discrete Laplace equation with given boundary conditions. The probability  $P$  of the pattern growth from  $(i, j)$  to  $(i', j')$  is expressed as follows;

$$P(i, j \rightarrow i', j') = \begin{cases} \frac{(\phi_{i',j'})^\eta}{\sum (\phi_{i',j'})^\eta} & \Delta\phi \geq \phi_b \\ 0 & \Delta\phi < \phi_b \end{cases} \quad (1)$$

Here, it is assumed that a power-law dependence with exponent  $\eta$  describes the relation between local field and probability. As will be discussed later,  $\eta$  is an important parameter to control the number of branches in the pattern. The indices  $(i, j)$  and  $(i', j')$  denote lattice coordinates

of points in the discharge pattern ( $\phi = 0$  V) and the candidate sites, respectively. Accordingly, the sum in the denominator of Eq. (1) refers to all of the possible growth sites  $(i', j')$  adjacent to  $(i, j)$ . Depending on this probability, a new point in the candidate site is randomly chosen and added to the discharge pattern. Using this new discharge pattern, the computation procedures are repeated. It should be noted that the pattern propagation is only possible if the electrical potential difference is greater than a breakdown voltage ( $\phi_b$ ).

Fig. 4 illustrates the configuration of the lattice for simulating surface tracking patterns based on DBM. Here the index of each cell (or box) indicates a discrete lattice coordinate. In this paper,  $300 \times 300$  lattices are utilized to compute the tracking pattern (Only a few lattices are shown in Fig. 4). As boundary conditions, the electrode with  $\phi = 0$  V is located at (150, 225) and the electrode with  $\phi = 1$  V is located at (150, 75).

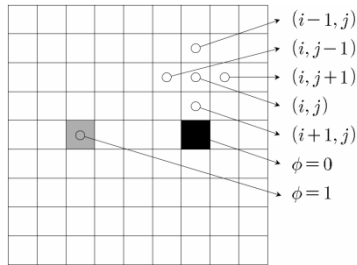


**Fig. 4.** Configuration of lattice for numerical computation

As mentioned previously, the pattern growth probability depends explicitly on the local electric potential which can be determined by a two-dimensional Laplace equation:

$$\frac{\partial^2 \phi}{\partial x^2} + \frac{\partial^2 \phi}{\partial y^2} = 0 \quad (2)$$

Using the centered finite difference method, it is possible to express the difference equation for Eq. (2) as follows;

$$\phi_{i,j} = \frac{(\phi_{i-1,j} + \phi_{i+1,j})/(\Delta x)^2 + (\phi_{i,j-1} + \phi_{i,j+1})/(\Delta y)^2}{2(1/(\Delta x)^2 + 1/(\Delta y)^2)} \quad (3)$$

where  $\Delta x$  (or  $\Delta y$ ) is the distance between adjacent lattice points on the  $x$  (or  $y$ ) axis. In the case of a uniform lattice configuration ( $\Delta x = \Delta y$ ), Eq. (3) can be written as

$$\phi_{i,j} = \frac{1}{4}(\phi_{i-1,j} + \phi_{i+1,j} + \phi_{i,j-1} + \phi_{i,j+1}) \quad (4)$$

where the indices  $i$  and  $j$  represent lattice coordinates in  $x$  and  $y$  directions, respectively. Eq. (4) means that the electric potential at a lattice point can be expressed as the average potential of the nearest neighbors of the point. Eq. (4)

can be solved by the Gauss-Seidel method which is the most commonly used iterative method. The formula of the Gauss-Seidel method for Eq. (4) can be expressed as

$$\tilde{\phi}_{i,j}^{(k+1)} = \frac{1}{4}(\phi_{i-1,j}^{(k+1)} + \phi_{i+1,j}^{(k)} + \phi_{i,j-1}^{(k+1)} + \phi_{i,j+1}^{(k)}) \quad (5)$$

where the index  $k$  denotes the iteration number. It is stressed that  $\phi_{i-1,j}^{(k+1)}$  and  $\phi_{i,j-1}^{(k+1)}$ , which have already been updated, are used to compute  $\tilde{\phi}_{i,j}^{(k+1)}$ . Although the electric potential can be computed using Eq. (5) on the basis of the Gauss-Seidel method, the convergence rate is not good. In order to accelerate the speed of solution convergence in Eq. (4), we use the successive over-relaxation (S.O.R) method together with the Gauss-Seidel method. The S.O.R formula for Eq. (5) is given by

$$\phi_{i,j}^{(k+1)} = (1 - \lambda)\phi_{i,j}^{(k)} + \frac{\lambda}{4}\tilde{\phi}_{i,j}^{(k+1)} \quad (6)$$

where  $\lambda$  is the over-relaxation parameter. The optimum value of  $\lambda$  is given by [11]

$$\lambda_{opt} = \frac{4}{2 + \sqrt{4 - [\cos(\pi/p) + \cos(\pi/q)]^2}} \quad (7)$$

where  $p$  and  $q$  are lattice lengths in the  $x$  and  $y$  directions, respectively. Since  $p = q = 300$  in this paper,  $\lambda_{opt} = 1.98$ .

Fig. 5 shows equipotential lines in the very beginning stage, which is determined using Eq. (6). Once the electric potential is obtained for all lattice points by means of the discrete Laplace equation, the probability function in Eq. (1) is used to choose the lattice points adjacent to the tracking pattern, which become a growth site. These points are added to the current pattern, giving a new pattern. The electric potential of all points in the new pattern are set to be 0 V as a new boundary condition for the computation of the next growth site. This DBM algorithm is repeatedly performed until the growth site reaches the positive potential ( $\phi = 1$  V) electrode. Fig. 6 illustrates examples of simulated electric equipotential line distribution and tracking patterns after the computation of  $N$  iteration in the DBM algorithm with a condition of  $\eta = 1$  and  $\phi_b = 2$  mV.

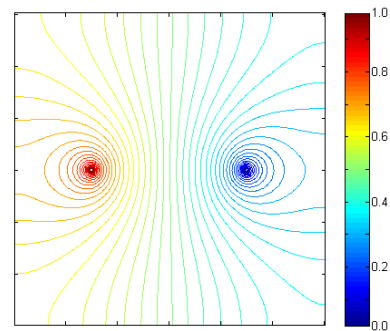


**Fig. 5.** Equipotential lines in the very beginning stage

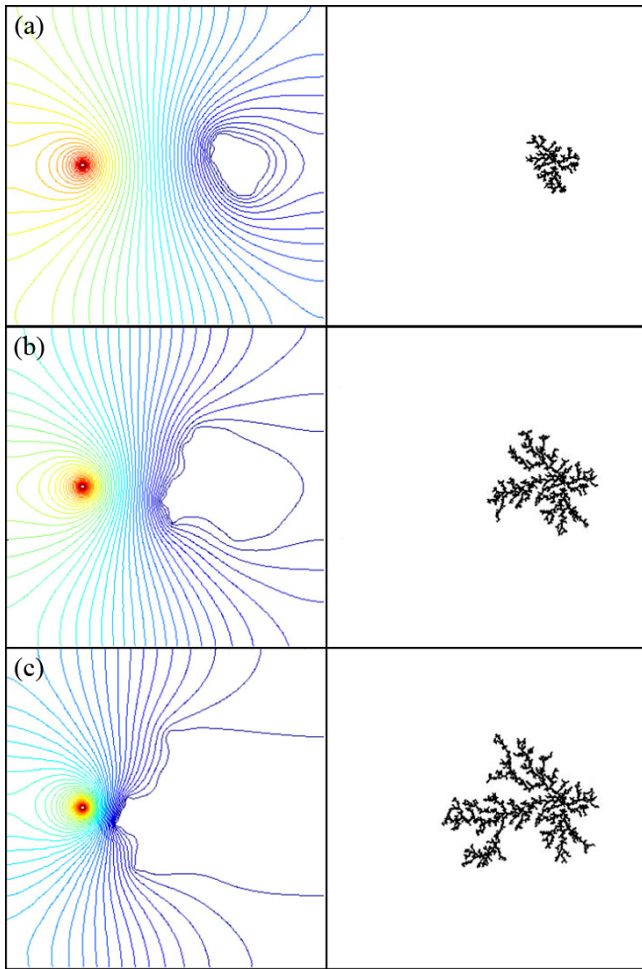


**Fig. 6.** Equipotential lines and tracking patterns after computation of N iteration: (a) N=1000 (b) N=2000 and (c) N=3000

### 3.2 Surface Tracking Patterns

It is obvious in Eq. (1) that the exponent  $\eta$  and the breakdown voltage  $\phi_b$  are essential factors to determine surface tracking patterns. In order to examine the effects of these factors on the pattern growth, the computations based on DBM are performed for four cases of  $\eta = 0.5$ ,  $\eta = 1.0$ ,  $\eta = 1.5$  and  $\eta = 2.0$ . In each case,  $\phi_b$  changes from 2 mV to 20 mV with a step size of 2 mV. Figs. 7-9 and 10 show simulated surface tracking patterns. In the case of low  $\eta$  and low  $\phi_b$  as shown in Fig. 7(a), the pattern appears to be nearly symmetrical and the density of tracking branches is very high. As  $\eta$  or  $\phi_b$  increases, however, the pattern tends to grow in the initial direction which has been chosen randomly in the very beginning stage. The random growth property of the pattern becomes more apparent at higher  $\eta$  or  $\phi_b$ . In addition, tracking branches get sparse as  $\eta$  or  $\phi_b$  increases.

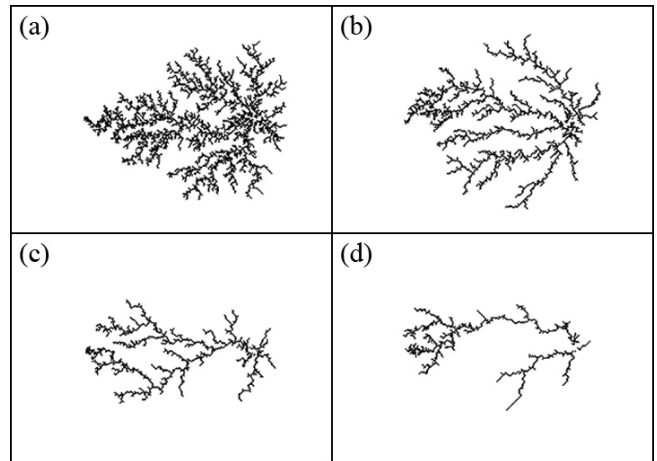


**Fig. 7.** Simulated surface tracking patterns for  $\eta = 0.5$  and  $\phi_b =$  (a) 2 mV, (b) 8 mV, (c) 14 mV and (d) 20 mV

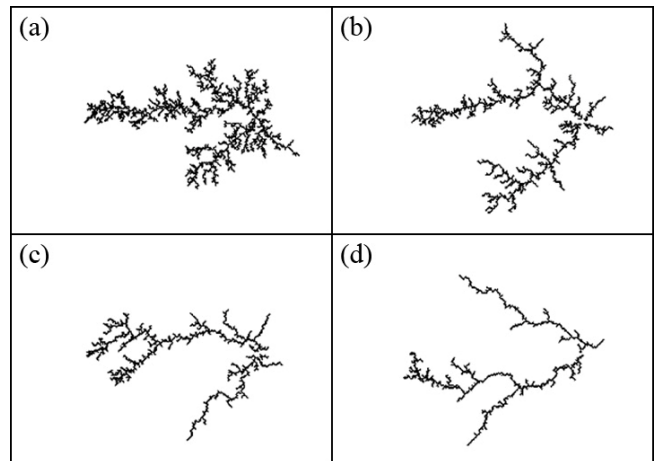


**Fig. 8.** Simulated surface tracking patterns for  $\eta = 1.0$  and  $\phi_b =$  (a) 2 mV, (b) 8 mV, (c) 14 mV and (d) 20 mV

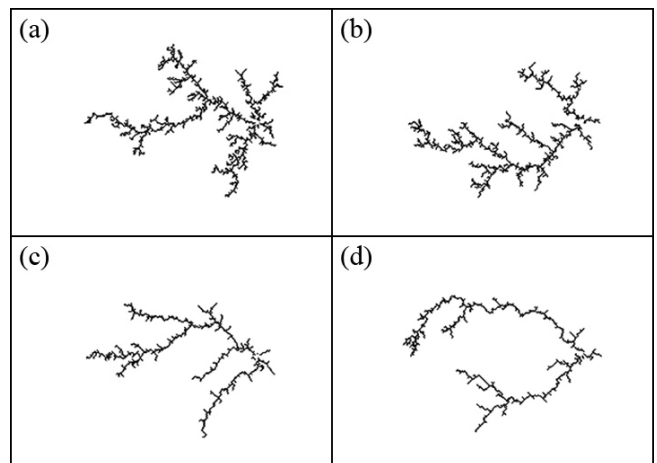


**Fig. 9.** Simulated surface tracking patterns for  $\eta = 1.5$  and  $\phi_b =$  (a) 2 mV, (b) 8 mV, (c) 14 mV and (d) 20 mV

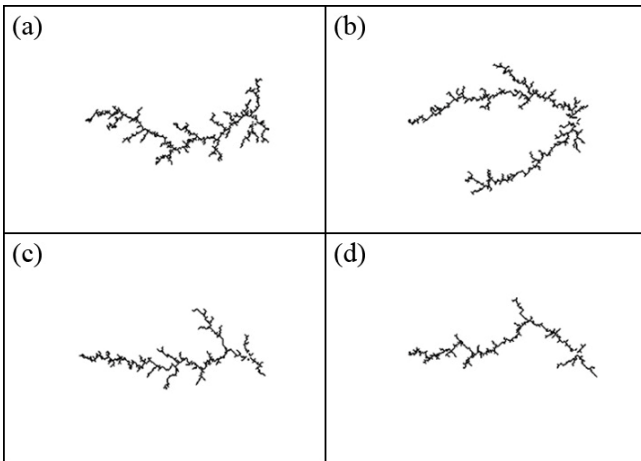


**Fig. 10.** Simulated surface tracking patterns for  $\eta = 2.0$  and  $\phi_b =$  (a) 2 mV, (b) 8 mV, (c) 14 mV and (d) 20 mV

#### 4. Fractal Analysis of Tracking Patterns

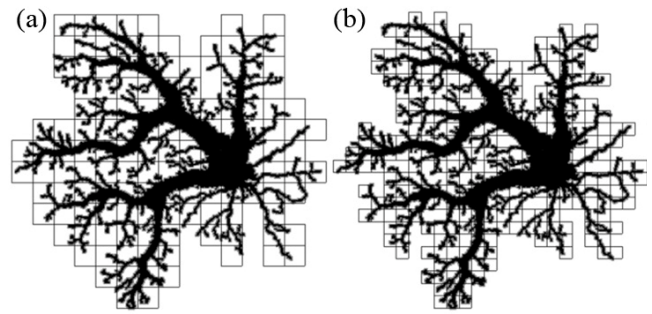
For the quantitative fractal analysis of the numerically generated surface tracking patterns in the previous section, we calculate the fractal dimension of the patterns. A variety of methods can be used to estimate the fractal dimension. These include the box counting method, the fractal measure relations, the correlation function, the distribution function and the power spectrum. [7] In this paper, the box counting method is employed to calculate the fractal dimension. Since the box counting method plays an essential role analyzing the tracking patterns, it is meaningful to explain how the box counting method works before proceeding to discussion of analysis results.

In the box counting method [7], a fractal pattern is completely covered by square boxes as shown in Fig. 11, and the following relation is satisfied;  $N(r) \sim r^{-D}$  where  $N(r)$  is the total number of covering boxes ( $r$  is the length of the box side) and  $D$  is the fractal dimension. Then, the fractal dimension can be expressed as

$$D = \frac{\log N(r)}{\log(1/r)} \quad (8)$$

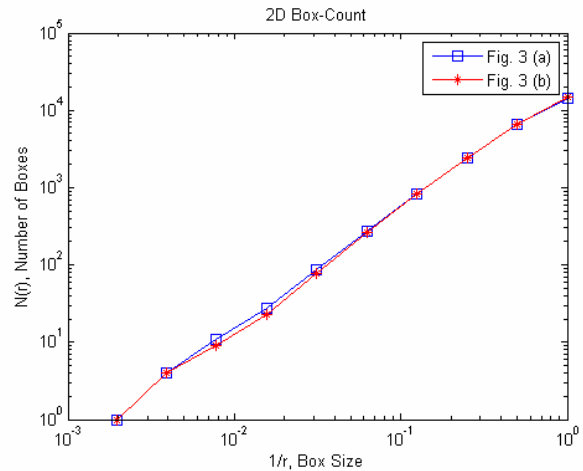
It is obvious from Eq. (8) that the fractal dimension can be determined by calculating the slope of a plot of  $\log N(r)$  versus  $\log(1/r)$ . It can be found from Fig. 12 that the mean fractal dimensions of the experimentally obtained tracking patterns are  $1.64 \pm 0.02$ .

Fig. 13 illustrates the fractal dimensions of the simulated tracking patterns, which are calculated using the box counting method. As can be seen, the fractal dimension varies in the interval ranging from 1.15 to 1.64, depending on  $\eta$  and  $\phi_b$ . As  $\eta$  increases at a constant  $\phi_b$  or  $\phi_b$  increases at a constant  $\eta$ , the fractal dimension decreases. Consider-



**Fig. 11.** Application of the box counting method to Pattern: (a) in Fig. 3, (a)  $r=40$  pixels and (b)  $r=20$  pixels

ing the fractal dimension of experimental data is  $\sim 1.64$ , it may be addressed that the pattern generated with  $\eta = 0.5$  and  $\phi_b = 2$  mV is nearly identical to Fig. 3 in terms of fractal dimension.



**Fig. 12.** Plot of  $\log N(r)$  versus  $\log(1/r)$  for the tracking patterns in Fig. 3

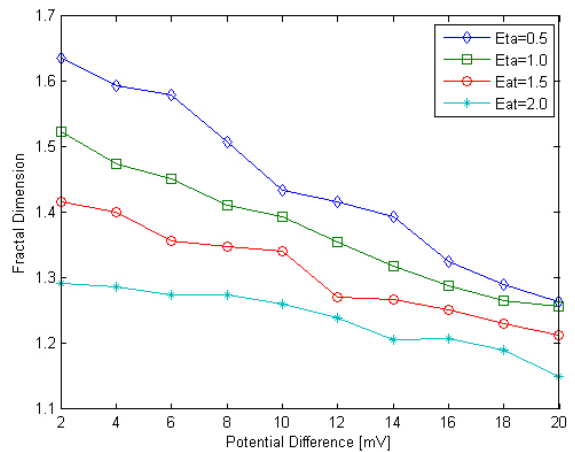


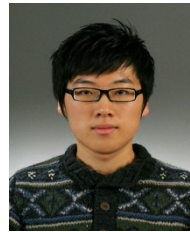
**Fig. 13.** Fractal dimensions of simulated tracking patterns.

## 5. Conclusion

DBM has been employed to numerically generate surface discharge tracking patterns with various values of  $\eta$  and  $\phi_b$ . The box counting method has been used to extract fractal dimensions of simulated tracking patterns. It is found from the simulation results that  $\eta$  and  $\phi_b$  have significant effects on the whole growth pattern of tracking channels and the density of tracking branches. That is, the appearance of the branches in the growth patterns is controlled by  $\eta$ . As  $\eta$  increases, the fractal nature of the pattern becomes weaker. In the comparison of experimental and simulated data, it is revealed that DBM is capable of generating the tracking patterns of which fractal structures are similar to those of experimentally obtained patterns when  $\eta = 0.5$  and  $\phi_b = 2$  mV.

## References

- [1] N. Yoshimura, M. Nishida and F. Noto, "Influence of electrolyte on tracking breakdown of organic insulation materials", *Trans. IEEE. EI*, vol. 16. pp. 510-519, 1981.
- [2] K. M. Song, Y. Roh, and H. R. Kwak, "Surface Discharge Characteristics of Phenolic Resin Treated by Heat and Its Structure Analysis", *J. KIIEE* vol.20, no.8, pp. 71-79 Sep. 2006.
- [3] S. T. Park and Y. Roh, "A Study on the Characteristics of Organic Insulating Materials Carbonized by a Leakage Current", *J. KIIEE* vol. 23, no.2, pp. 161-167 Feb. 2009.
- [4] Kebbabi and Beroual, "Fractal analysis of creeping discharge patterns propagating at solid/liquid interfaces: influence of the nature and geometry of solid insulators", *J. Phys. D: Appl. Phys.* **39** (2006) 177-183
- [5] V Rajini and K Udaya Kumar, "Surface tracking in polymers: a pattern discrimination technique using fractals", *J. Phys. D: Appl. Phys.* **39** (2006) 3695-3701
- [6] Candela R, Mirolli G and Schifani R, "PD recognition by means of statistical and fractal parameters and a neural network" *IEEE Trans. Electr. Insul.* **7** (2000) 87-94K.
- [7] Kudo, "Fractal Analysis of Electrical Trees", *IEEE Transactions on Dielectrics and Electrical Insulation* **5**, (1998) 713-727
- [8] T. A. Witten, Jr. and L. M. Sander, "Diffusion-Limited Aggregation, a Kinetic Critical Phenomenon", *Physical Review Letters*, vol.47, no.10, pp. 1400-1403, Nov. 1981.
- [9] L. Niemeyer, L. Pietronero, and H. J. Wiesmann, "Fractal Dimension of Dielectric Breakdown", *Physical Review Letters*, vol.52, n0.12, pp.1033-1036, March 1984
- [10] N. Femia, L. Niemeyer and V. Tucci, "Fractal characteristics of electrical discharges: experiments and simulation", *J. Phys. D: Appl. Phys.*, vol. 26, pp.619-627, 1993.
- [11] J. H. Mathews and K. D. Fink, "Numerical Methods using Matlab", Pearson Prentice Hall, 2004



**Jun-Won Kim** He received his B.S. degrees in Electrical Engineering from Soongsil University in 2009. He is currently an M.S. course in Electrical Engineering from Soongsil University. His research interests include fractal and high voltage discharges.



**Young-Su Roh** He received his B.S. and M.S. degrees in Electrical Engineering from Seoul National University in 1984 and 1986, respectively. He received a Ph.D. degree in Applied Science from the University of California, Davis in 2001.

From 1988 to 1996, he worked at the Korea Electricity Research Institute. He is currently an Associate Professor at the Department of Electrical Engineering at Soongsil University. His research interests include plasma physics, nuclear fusion, and electrical discharges.